J. Nannoplankton Res. **31** (1), 2010, pp.5-10 © 2010 International Nannoplankton Association, Inc.
ISSN 1210-8049 Printed by The Sheridan Press, Hanover, PA, USA

A new calcareous nannofossil species of the genus *Sphenolithus* from the Middle Eocene (Lutetian) and its biostratigraphic significance

Jamie L. Shamrock
Geosciences Department, University of Nebraska-Lincoln, 214 Bessey Hall, PO Box 880340, Lincoln, Nebraska; jamie.shamrock@huskers.unl.edu (currently, jamie.l.shamrock@exxonmobil.com)

Manuscript received 13th August, 2009; revised manuscript accepted 14th March, 2010

Abstract A high-resolution biostratigraphic study of Eocene calcareous nannofossils from Ocean Drilling Program (ODP) Leg 122 Hole 762C (Exmouth Plateau, western Australian shelf) has identified a new nannofossil species, *Sphenolithus perpendicularis* sp. nov. This species bears a double apical spine, similar to both *S. furcatolithoides* and *S. capricornutus*, but is distinguished by both optical properties and stratigraphic range. The range and distribution of *S. perpendicularis* sp. nov. is limited to nannofossil zone CP13a (equivalent to NP15a) at Hole 762C, and verified in sediments from Deep Sea Drilling Project Leg 77 Hole 538A and ODP Leg 159 Hole 960A. This suggests both a global distribution and a reasonably synchronous stratigraphic range. The optical properties and stratigraphic range of *S. perpendicularis* sp. nov. may suggest a taxonomic relationship to the *S. anarrhopus-editus-spiniger* lineage. This new species, in conjunction with *S. furcatolithoides* and *S. cuniculus*, may provide an alternate means for subdividing nannofossil zone CP13 (NP15).

Keywords Calcareous nannofossils, biostratigraphy, *Sphenolithus*, Eocene, taxonomy, Ocean Drilling Program

1. Introduction

A new species of calcareous nannofossil, *Sphenolithus perpendicularis* sp. nov., was identified during a high-resolution biostratigraphic study of Eocene open-ocean sediments from Ocean Drilling Program (ODP) Leg 122 Hole 762C (Figure 1). *S. perpendicularis* sp. nov. shows a unique morphology and is moderately abundant over its notably short stratigraphic range, giving potential for use in nannofossil biostratigraphy. This utility is enhanced particularly in sections where *Nannotetrina* spp. are rare to absent, as is the case at Hole 762C. *S. perpendicularis* sp. nov., along with the morphologically-related species *S. furcatolithoides* and *S. cuniculus*, show considerable potential as alternate subzonal markers within CP13 (of Okada & Bukry, 1980; equivalent to NP15 of Martini, 1971).

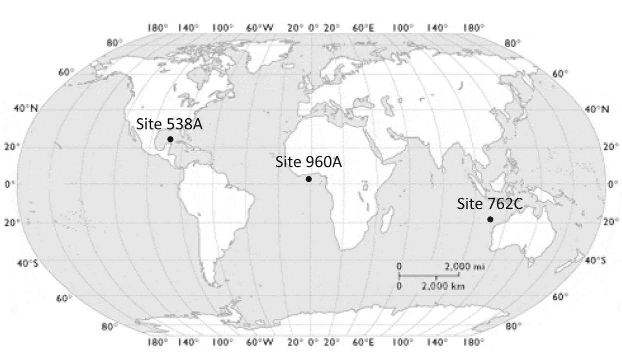

Figure 1: Geographical distribution of the three localities examined

2. Materials and Methods

The primary locality in this study is ODP Leg 122 Hole 762C, located on the central Exmouth Plateau (19˚53.23'S, 112˚15.24'E), separated from the Australian Northwest Shelf by the Kangaroo Syncline (von Rad *et al*., 1992). Eocene pelagic sediments from this locality consist of white to green-grey, calcareous oozes, chalks and marls, indicating a mature, open-ocean setting (von Rad *et al*., 1992). Hole 762C was drilled in 1360m of water, with decompacted burial curves signifying little change in depth since the time of original deposition (Haq *et al*., 1992). Calcareous nannofossils are moderately to well preserved, with deposition well above the carbonate compensation depth. Secondary localities used in this study include Deep Sea Drilling Program (DSDP) Leg 77 Hole 538A (Buffler *et al*., 1984) in the eastern Gulf of Mexico (23˚50.95'N, 85˚09.93'W) and ODP Leg 159 Hole 960A (Mascle *et al*., 1996), Ivory Coast, Ghana (3˚34.979'N, 2˚44.009'W) (Figure 1).

Smear-slide preparation for Hole 762C followed standard techniques, as described by Bown & Young (1998) and slides were mounted using Castolite AP Crystal Clear Polyester Resin. Smear slides from Holes 538A and 960A were prepared previously for the University of Nebraska-Lincoln Micropaleontology Repository using the double slurry method (Watkins & Bergen, 2003) and mounted with Norland 61 optical adhesive. Smear-slides were examined at 1250x magnification with an Olympus BX51 transmitting light microscope under plane parallel light (PL), cross-polarised light (XPL), and a one-quarter λ mica interference plate. Univariate analysis of key morphological characteristics was conducted using PAST (Hammer *et al*., 2001).

3. Abundance and distribution

The relative abundance of *Sphenolithus perpendicularis* sp. nov. was documented throughout its observed range in Core 16 of Hole 762C (Figure 2). Though numerically few (1 specimen per 2-10 fields of view), this species shows a notable increase in abundance near the central portion of its range (Figure 2). The first occurrence (FO) of *S. perpendicularis* sp. nov. is located near the base of nannofossil subzone CP13a (equivalent to NP15), marked by the FO of *Nannotetrina fulgens (*syn. *N. quadrata, N. alata)* (Figure 3). The last occurrence (LO) is located near the top of CP13a, marked by the FO of *Chiasmolithus gigas*.

Following initial identification at Hole 762C, *S. perpendicularis* sp. nov. was also observed in DSDP Leg 77 Hole 538A-17-4, 111-113cm in the eastern Gulf of Mexico, as well as in ODP Leg 159 Hole 960A-14CC along the Ivory Coast, Ghana (Figure 1). The biostratigraphic zonations for these samples was derived from Lang & Watkins (1984) and Shafik *et al*. (1998), respectively. The presence of *S. perpendicularis* sp. nov. in the Indian and Atlantic Oceans, as well as the Gulf of Mexico, indicates a widely distributed species; however, all sites were located below 25˚ palaeolatitude, which may indicate a restriction to tropical to subtropical water-masses.

4. Morphology and lineage

Sphenolithus perpendicularis sp. nov. consists of a small to medium sphenolith base with two tapering, apical spines that diverge to ~90˚ just above the basal cycles. Standard sphenolith morphological terms are shown in Figure 4.

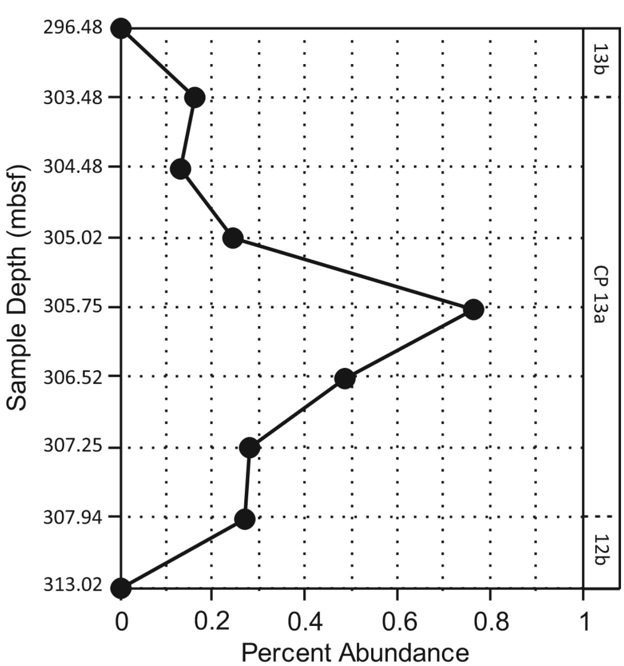

Figure 2: Graph showing percent abundance of *S. perpendicularis* sp. nov. to total nannofossil assemblage (total *S. perpendicularis* per traverse/total nannofossils per traverse x 100). *S. perpendicularis* appears to range throughout CP13a

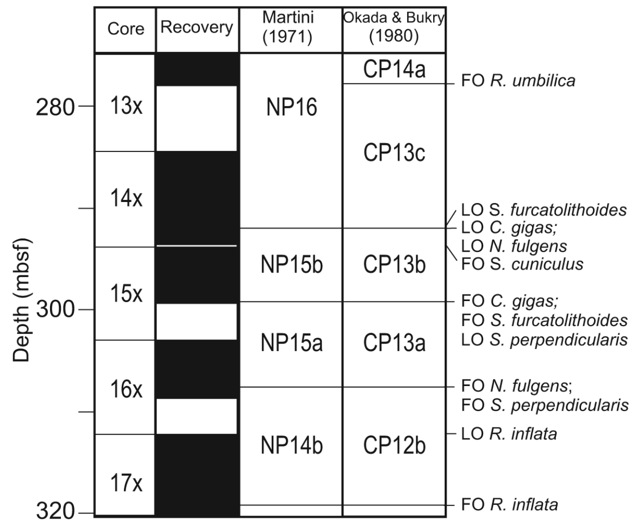

Figure 3: Nannofossil biostratigraphic scheme for the studied interval at Hole 762C, showing sample depth, core interval, core recovery, NP and CP (sub)zonal markers, along with appearance of key *Sphenolithus* species. See Table 1 for detailed interval data

Though *S. perpendicularis* sp. nov. shares a dual apical spine with *S. furcatolithoides*, these species differ in significant ways: *S. perpendicularis* sp. nov. shows a wide angle of divergence ($\mu = 96.1˚$, N = 30) between the apical spines, which occurs just above a more prominent lateral cycle, and appears stratigraphically restricted to subzone CP13a. *S. furcatolithoides* shows a distinctly acute angle of divergence that occurs more distally from a reduced lateral cycle. In addition, *S. furcatolithoides* does not appear until CP13b at Hole 762C. As the FO of *S. furcatolithoides* is shown near the base of NP15 (CP13) in Perch-Nielsen (1985, fig.69), *S. perpendicularis* sp. nov. has likely been grouped with the former, though it is now apparant that these two distinct species show little, if any, stratigraphic overlap. The precise degree of overlap cannot be determined at Hole 762C due to only partial recovery near the CP13a/13b boundary. The true stratigraphic relationships will likely be refined in a more continuous section through the CP13a/13b boundary.

The morphological trend from *S. perpendicularis* sp. nov. to *S. furcatolithoides* continues with *S. cuniculus*, wherein the base is further reduced, the angle between the apical spines becomes more acute, and divergence of the spines occurs more distally than in *S. furcatolithoides*. Key characteristics used to identify these three species can be seen when aligned at 0˚ as well as at 45˚ under XPL, and are shown in Figure 5 and Plate 1.

Perch-Nielsen (1985, fig.69) hypothesised the evolution of *S. furcatolithoides* from the *S. anarrhopus*-*S. orphanknollensis*-*S. spiniger* lineage. Evidence from this study indicates that *S. furcatolithoides* did not arise directly from *S. spiniger*, but more likely from the short-lived *S. perpendicularis* sp. nov. (Figure 6). If *S. perpendicularis* sp. nov. is an ancestral species of *S. furcatolithoides,* then this new species may also be related to this lineage. This re-

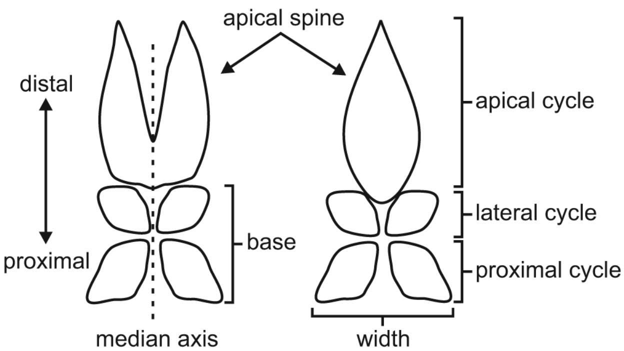

Figure 4: Schematic diagram showing basic sphenolith morphological terms. See also Young *et al*. (1997, fig.12) and Perch-Nielsen (1985, fig.69)

lationship would require some reorganisation of the crystal units, so that the small central spine of *S. spiniger* is further reduced and two divergent units, birefringent at 0˚, are enlarged. This issue is unlikely to be resolved without further investigation using a scanning electron microscope (SEM).

S. perpendicularis sp. nov. is also morphologically similar to *S. capricornutus*, in that both bear widely-divergent apical spines that are highly birefringent when aligned with the polarisers. There are notable differences between these species when oriented at 45˚ (Figure 5), with *S. perpendicularis* sp. nov. having four birefringent crystals in the proximal and lateral cycles and *S. capricornutus* having only two crystals birefringent, in the proximal cycle only. In addition, there is a prominent stratigraphic separation of more than 15Myr: *S. perpendicularis* sp. nov. appears to be restricted to CP13a (NP15; Middle Eocene, Lutetian), while *S. capricornutus* first appears in the latest Oligocene (Chattian), in CP19b (NP25). If *S. perpendicularis* sp. nov. does indeed develop from *S. spiniger*, and the remainder of the lineage given by Perch-Nielsen (1985) is correct, then the apical spine morphology associated with *S. perpendicularis* sp. nov. and *S. capricornutus* must have developed iteratively within two distinct lineages.

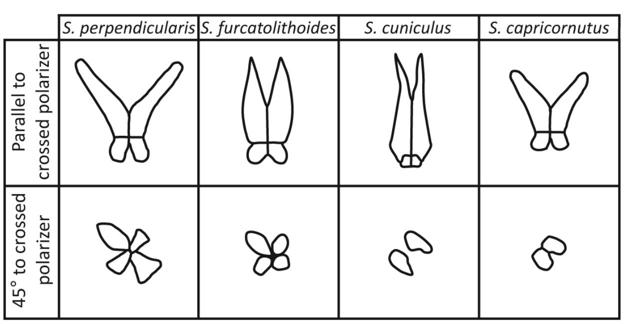

Figure 5: Stylised drawing showing birefringence and extinction patterns of *Sphenolithus perpendicularis* sp. nov., *S. furcatolithoides, S. cuniculus* and *S. capricornutus* aligned at 0˚ and 45˚ to crossed polarisers

5. Biostratigraphic significance

Currently, nannofossil biozone CP13 is divided into three subzones, where the FO of *Nannotetrina fulgens*, FO of *Chiasmolithus gigas* and LO of *C. gigas* mark the bases of CP13a, CP13b and CP13c, respectively (Figure 3, Table 1). As stated above, and as noted by Perch-Nielsen (1985), *N. fulgens* is rare to absent in many sections, often reducing its biostratigraphic utility. As a result, many nannofossil workers employ the LO of *Rhabdosphaera inflata* as a secondary marker for the base of CP13a. Although this has provided a useful alternative, *R. inflata* can also be rare, leading to an ambiguous LO. *C. gigas* may also be rare in some localities, such as Hole 762C.

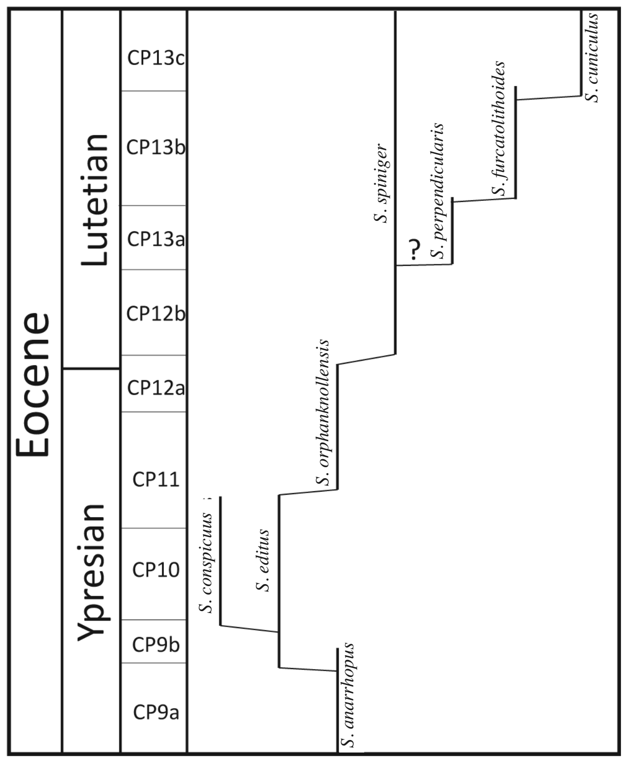

Figure 6: Tentative evolutionary lineage of *Sphenolithus,* integrating *S. perpendicularis* sp. nov. and *S. cuniculus* (modified from Perch-Nielsen, 1985, fig.69)

Where the historic (sub)zonal markers are rare to absent, *S. perpendicularis* sp. nov., *S. furcatolithoides* and *S. cuniculus* may prove to be useful substitutes. The FO of *S. perpendicularis* sp. nov. closely approximates the base of CP13a, as it coincides with the FO of *N. fulgens* and occurs just above the LO of *R. inflata* at Hole 762C (Figure 3, Table 1). The LO of *S. perpendicularis* sp. nov. occurs just below the FO of *C. gigas*, at the base of CP13b, which also marks the FO of *S. furcatolithoides*. Bown (2005, fig.1) also showed the FO of *S. furcatolithoides* within CP13b, though above the FO of *C. gigas*. The FO of *S. cuniculus* occurs in CP13b, though near the top of this subzone. This range was confirmed by the short overlap with *C. gigas,* facilitated by the highly-expanded section at Hole 762C. A short stratigraphic overlap was also observed between *S. furcatolithoides* and *S. cuniculus*. This overlap of *C. gigas*, *S. furcatolithoides* and *S. cuniculus* can be used to

Species	FO interval	Depth mbsf	LO interval	Depth mbsf	Zonal marker
Rhabdosphaera inflata	17-5, 49.5-50.5cm	318.995	17-1, 45-46cm	113.01	FO base CP12b/NP14b
Nannotetrina fulgens	16-4, 45-46cm	307.95	14-6, 50-51cm	292.00	FO base CP13a/NP15a LO base NP16
Sphenolithus perpendicularis	16-4, 45-46cm	307.95	16-1, 48-49cm	303.48	FO approximates base of CP13a/NP15a
Chiasmolithus gigas	15-3, 48-49cm	296.48	14-6, 50-51cm	292.00	FO base CP13b/NP15b LO base CP13c/NP15c
Sphenolithus furcatolithoides	15-3, 48-49cm	296.48	14-4, 55-56cm	289.05	FO approximates base of CP13b/NP15b LO near base CP13c
Sphenolithus cuniculus	15-1, 48-49cm	293.98	not encountered		
Reticulofenestra umbilica	13-1, 50-51cm	275.00	not encountered		FO base CP14a

Table 1: Sample intervals and depths of FOs and LOs of key biostratigraphic markers and species of *Sphenolithus* from Hole 762C

identify the uppermost portion of CP13b. The LO of *S. furcatolithoides* occurs just slightly above the LO of *C. gigas* in Hole 762C, so that only *S. cuniculus* remains throughout CP13c. In summation, the stratigraphic data provided from Hole 762C (Figure 3, Table 1) indicates potential for secondary markers, using *S. perpendicularis* sp. nov., *S. furcatolithoides* and *S. cuniculus* as a means to approximate subzones within CP13.

6. Systematic palaeontology

All figured specimens and type species are housed in the Micropaleontology Collections at the University of Nebraska-Lincoln. Species description uses terms recommended by Young *et al*. (1997). Basic sphenolith terminology is illustrated in Figure 4. Light photomicrographs of selected specimens illustrated in Plate 1 were taken at the same magnification.

Order DISCOASTERALES **Hay, 1977**
Family **SPHENOLITHACEAE** Deflandre *in* Grassé, 1952
Genus *Sphenolithus* Deflandre *in* Grassé, 1952

Sphenolithus perpendicularis sp. nov.

Pl.1, figs 1-6. **Derivation of name**: From the Latin '*perpendicularis*', referring to the near-perpendicular angle between the apical spines immediately above the proximal base. **Diagnosis**: Sphenolith with a small- to medium-sized base, bearing two tapering, apical spines that diverge to ~90° just above the basal cycles. **Description**: Proximal cycle consisting of about 10 elements, greater than half the length of the base, supporting a lateral cycle that is equal to or less than the width of the proximal cycle, giving a generally square outline. The base supports two prominent apical spines centered about the median axis, which are widely divergent just above the base. Measurement of 30 specimens yields a mean angle of divergence of 96.1°. These spines may be more than twice the length of the base in well-preserved specimens, but may break or dissolve in more poorly-preserved forms. When the long axis is oriented at 0° under XPL, the outer elements of the proximal base, upper lateral cycle and apical spines are highly birefringent. When oriented at 45°, the central elements of the proximal base and the lateral cycle are highly birefringent, with the prominent apical spines being extinct (Figure 5). Specimens may also show an enlarged element in the upper cycle, centered about the median axis, which projects above the base between these larger spines. In less well-preserved specimens, this enlarged element may approximate the length of the spines, giving specimens a more tricuspid appearance. Imaging of these specimens was difficult due to poor preservation and high birefringence. **Differentiation**: *Sphenolithus perpendicularis* can be differentiated from *S. capricornutus* by the birefringence pattern observed at 45°, as shown in Figure 5. These species can be further distinguished by a prominent stratigraphic separation of more than 15Myr. *S. perpendicularis* may be differentiated from *S. furcatolithoides* by the significantly wider angle of divergence of the spines. In addition, there appears to be little, if any, stratigraphic overlap of these two species. **Dimensions**: (N = 30 for base width, height and interior angle). Base width: 3.2μm (min.), 4.8μm (max.), 4.0μm (mean), 0.08 (std. error), 0.21 (variance). Base height: 3.2μm (min.), 4.8μm (max.), 4.0μm (mean), 0.08 (std. error), 0.21 (variance). Apical spine interior angle: 85.5° (min.), 115.8° (max.), 96.1° (mean), 1.3 (std. error), 0.51 (variance). Spine length: 2.0 to 8.5μm, dependant on preservation. **Holotype**: Pl.1, fig.1. **Paratype**: Pl.1, fig.2. **Type locality**: ODP Leg 122, Exmouth Plateau, western Australia. **Type level**: Middle Eocene (Lutetian), Hole 762C-16-2, 125-126cm. **Occurrence**: CP13a; 762C-16-4, 45-46cm to 762C-15-3, 48-49cm.

Plate 1

Scale-bars = 5μm
For each specimen, even numbers - specimens aligned with polarisers, odd numbers - 45° to polarisers

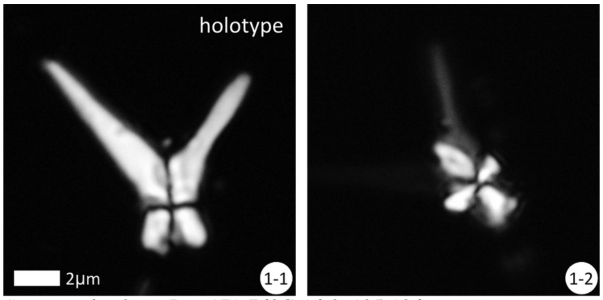

S. perpendicularis Leg 171-762C-16-2, 125-126cm

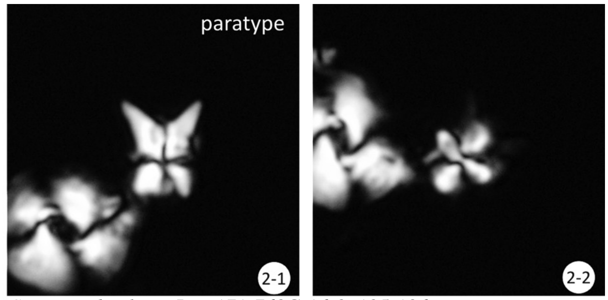

S. perpendicularis Leg 171-762C-16-2, 125-126cm

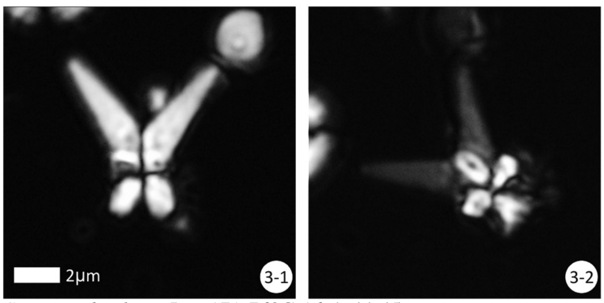

S. perpendicularis Leg 171-762C-16-4, 44-45cm

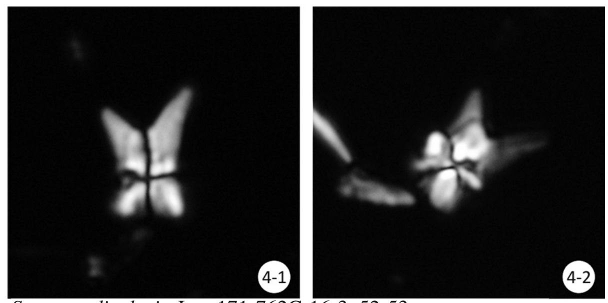

S. perpendicularis Leg 171-762C-16-3, 52-53cm

S. perpendicularis Leg 171-762C-16-2, 125-126cm

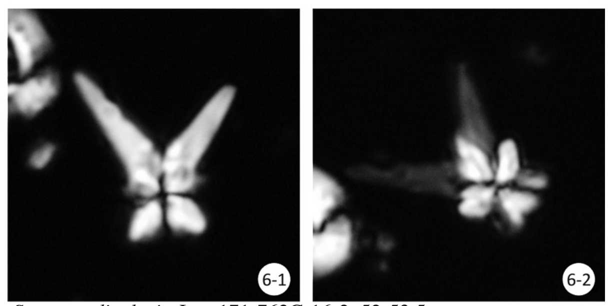

S. perpendicularis Leg 171-762C-16-2, 52-53.5cm

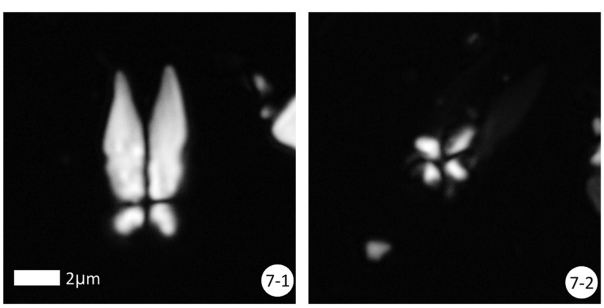

S. furcatolithoides Leg 171-762C-15-1, 48-49cm

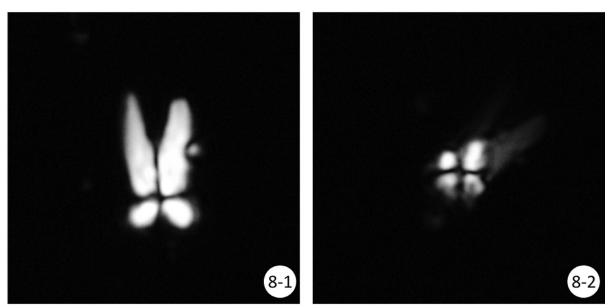

S. furcatolithoides Leg 171-762C-15-2, 125-126cm

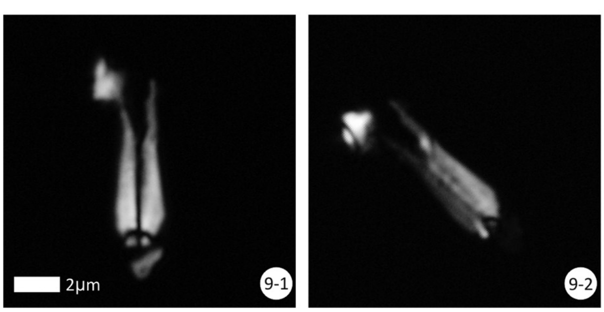

S. cuniculus Leg 171-762C-14-4, 55-56cm

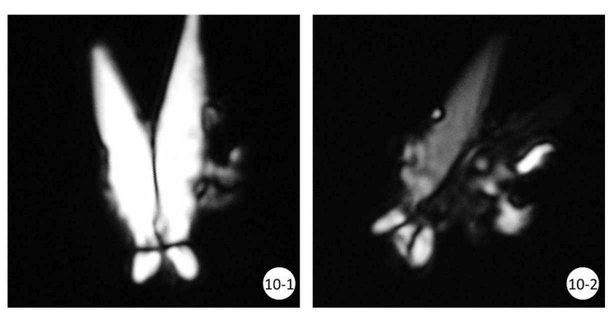

S. cuniculus Leg 171-762C-12-4, 50-51cm

Appendix

Chiasmolithus gigas (Bramlette & Sullivan, 1961) Radomski, 1968
Nannotetrina fulgens (Stradner *in* Martini & Stradner, 1960) Achuthan & Stradner, 1969
Rhabdosphaera inflata Bramlette & Sullivan, 1961 (= *Blackites inflata*)
Sphenolithus capricornutus Bukry & Percival, 1971
Sphenolithus cuniculus Bown, 2005
Sphenolithus furcatolithoides Locker, 1967
Sphenolithus spiniger Bukry, 1971

Acknowledgements

This research used samples and data provided by the DSDP and ODP. The DSDP and ODP are sponsored by the National Science Foundation (NSF) and participating countries, under the management of Joint Oceanographic Institutions (JOI), Inc. The author would like to thank David Watkins (University of Nebraska-Lincoln) and Kurt Johnston (ExxonMobil), Jackie Lees, Tom Dunkley-Jones (Imperial College London), and one anonymous reviewer for their collaboration and revisions, which greatly improved this manuscript.

References

Achuthan, M.V. & Stradner, H. 1969. Calcareous nannoplankton from the Wemmelian stratotype. *In*: P. Brönnimann & H.H. Renz (Eds). *Proceedings, First International Conference on Planktonic Microfossils, Geneva*, **1**: 1-13.

Bown, P.R. 2005. Paleogene calcareous nannofossils from the Kilwa and Lindi areas of coastal Tanzania (Tanzania Drilling Project 2003-4). *Journal of Nannoplankton Research*, **27**(1): 21-95.

Bown, P.R. & Young, J.R. 1998. Techniques. *In*: P.R. Bown (Ed.). *Calcareous Nannofossil Biostratigraphy*. Kluwer Academic Publishers, London: 16-28.

Bramlette, M.N. & Sullivan, F.R. 1961. Coccolithophorids and related nannoplankton of the early Tertiary in California. *Micropaleontology*, **7**: 129-174.

Buffler, R.T. *et al*. 1984. *Deep Sea Drilling Program, Initial Reports*, **77**. Washington (US Govt. Printing Office): 738pp.

Bukry, D. 1971. Cenozoic calcareous nannofossils from the Pacific Ocean. *Transactions of the San Diego Society of Natural History*, **16**: 303-27.

Bukry, D. & Percival, S.F. 1971. New Tertiary calcareous nannofossils. *Tulane Studies in Geology and Paleontology*, **8**(3): 123-146.

Deflandre, G. 1952. Classe des Coccolithophoridés (Coccolithophoridae Lohmann, 1902). *In*: P.P. Grassé (Ed.). *Traité de Zoologie. Anatomie, Systématique, Biologie,* **1** (pt.1). *Phylogenie. Protozoaires: generalité. Flagellés*. Masson & Cie, Paris: 439-470.

Hammer, Ø., Harper, D.A.T. & Ryan, P.D. 2001. PAST: Paleontological Statistics Software Package for Education and Data Analysis. *Palaeontologia Electronica*, **4**(1): 9pp. (http://palaeo-electronica.org/2001_1/past/issue1_01.htm)

Haq, B.U. *et al*. 1992. Evolution of the Central Exmouth Plateau: A post-drilling perspective. *Proceedings of the Ocean Drilling Program, Scientific Results,* **122**: 801-816.

Hay, W.W. 1977. Calcareous nannofossils. *In*: A.T.S. Ramsay (Ed.). *Oceanic Micropaleontology*. Academic Press, New York: 1055-2000.

Lang, T.H. & Watkins, D.K. 1984. Cenozoic calcareous nannofossils from Deep Sea Drilling Project Leg 77: biostratigraphy and delineated hiatuses. *Initial Reports of the Deep Sea Drilling Program*, **77**: 629-648.

Locker, S. 1967. Neue Coccolithophoriden aus dem Alttertiär Norddeutschlands. *Geologie*, **16**: 361-364.

Martini, E. 1971. Standard Tertiary and Quaternary calcareous nannoplankton zonation. *In*: A. Farinacci (Ed.). *Proceedings of the 2nd Planktonic Conference, Roma 1970. Tecnoscienza, rome*, **2**: 739-785.

Martini, E. & Stradner, H. 1960. *Nannotetraster*, eine stratigraphisch bedeutsame neue Discoasteridengattung. *Erdoël-Zeitschrift*, **8**: 266-270.

Mascle, J. *et al*. 1996. *Proceedings of the Ocean Drilling Program, Initial Reports,* **159**. College Station, TX (Ocean Drilling Program).

Okada, H. & Bukry, D. 1980. Supplementary modification and introduction of code numbers to the low-latitude coccolith biostratigraphic zonation (Bukry, 1973; 1975). *Marine Micropaleontology,* **5**: 321-325.

Perch-Nielsen, K. 1985. Cenozoic calcareous nannofossils. *In*: H.R. Bolli, J.B. Saunders & K. Perch-Nielsen (Eds). *Plankton Stratigraphy*. Cambridge University Press, Cambridge: 427-554.

von Rad, U. *et al*. 1992. Rift-to-drift history of the Wombat Plateau, northwestern Australia: Triassic to Tertiary Leg 122 results. *Proceedings of the Ocean Drilling Program, Scientific Results*, **122**: 765-800.

Radomski, A. 1968. Calcareous nannoplankton zones in Palaeogene of the western Polish Carpathians. *Rocz. Pol. Tow. Geol.,* **38**: 545-605.

Shafik, S., Watkins, D.K. & Shin, I.C. 1998. Calcareous nannofossil Paleogene biostratigraphy, Côte D'Ivoire-Ghana Marginal Ridge, eastern Equatorial Atlantic. *Proceedings of the Ocean Drilling Program, Scientific Results*, **159**: 413-431.

Watkins, D.K. & Bergen, J.A. 2003. Late Albian adaptive radiation of the calcareous nannofossil genus *Eiffellithus*. *Micropaleontology*, **49**: 231-252.

Young, J.R., Bergen, J.A., Bown, P.A., Burnett, J.A., Fiorentino, A., Jordan, R.W., Kleijne, A., van Niel, B.E., Romein, A.J.T. & von Salis, K. 1997. Guidelines for coccolith and calcareous nannofossil terminology. *Palaeontology*, **40**(4): 875-912.